Arc-continent collision" of the Aleutian-Komandorsky arc into Kamchatka: insight into Quaternary tectonic segmentation through Pleistocene marine terraces and morphometric analysis of fluvial drainage

Kevin Pedoja, Christine Authemayou, T. K. Pinegina, J. Bourgeois, M. Nexer, Bernard Delcaillau, Vincent Regard

"Arc-continent collision" of the Aleutian-Komandorsky arc into Kamchatka: Insight into Quaternary tectonic segmentation through Pleistocene marine terraces and morphometric analysis of fluvial drainage

K. Pedoja,[1,2,3] C. Authemayou,[4] T. Pinegina,[5] J. Bourgeois,[6] M. Nexer,[1,2,3] B. Delcaillau,[1,2,3] and V. Regard[7,8,9]

Received 14 September 2012; revised 11 May 2013; accepted 17 May 2013; published 20 July 2013.

[1] At the NW corner of the Pacific region, just south of the Kamchatsky Peninsula, the northern tip of the Pacific plate subduction and associated volcanic arc interacts with the western end of the Aleutian-Komandorsky dextral transform plate boundary and associated arc. Study of both Holocene and Pleistocene sequences of uplifted marine terraces and also of fluvial drainage patterns on the Kamchatsky Peninsula allows us to highlight active tectonics produced by complex plate interaction. Our results show that the central eastern coast of the peninsula is currently divided into four different zones consisting in uplifted blocks associated with various uplift rates in front of a fold-and-thrust zone to the west. Our main tectonic benchmark—the altitude of the shoreline correlated to the Last Interglacial Maximum (Marine Isotopic Stage 5e)—yields late Pleistocene uplift rates ranging from 0.2 to 2.74 mm/yr. One of the main active faults bounding the coastal blocks is dextral and is interpreted as a prolongation of an offshore fault of the Aleutian-Komandorsky dextral transform plate boundary. We suggest that structures on the Kamchatsky Peninsula accommodate a part of the transform motion, but that mainly, the arc-continent collision of the Aleutian arc against Kamchatka produces a "bulldozer" effect on the Kamchatsky Peninsula.

Citation: Pedoja, K., C. Authemayou, T. Pinegina, J. Bourgeois, M. Nexer, B. Delcaillau, and V. Regard (2013), "Arc-continent collision" of the Aleutian-Komandorsky arc into Kamchatka: Insight into Quaternary tectonic segmentation through Pleistocene marine terraces and morphometric analysis of fluvial drainage, *Tectonics*, *32*, 827–842, doi:10.1002/tect.20051.

1. Introduction

[2] The NW corner of the Pacific is one of the most tectonically active and complex areas of the circum-Pacific. In this region, the Pacific oceanic plate is subducting along the Kuril-Kamchatka trench at an estimated rate of 80 mm/yr (Model Nuvel 1A) [*DeMets et al*., 1994] and ends along the south side of the Kamchatsky Peninsula (Figure 1). [The Kamchatsky Peninsula, not to be confused with the entire Kamchatka Peninsula (a continental-scale peninsula, i.e., >1000 km long), is sometimes called the Kamchatsky Mys Peninsula or the Cape Kamchatsky Peninsula, where Kamchatsky Mys (Cape) is a subfeature of the Kamchatsky Peninsula (Figure 2).] Just north of the subduction zone, the Aleutian-Komandorsky arc, located along the Aleutian-Komandorsky dextral transform plate boundary, is impinging on Kamchatka at a short-term (GPS-measured) rate of about 40 mm/yr [*Gordeev et al*., 2001]. Bering Island is moving about 35–50 mm/yr NW relative to North America (Figure 1), and Krutoberegovo, on the west side of the Kamchatsky Peninsula, is moving about 8–15 mm/yr (Figure 2) [e.g., *Bürgmann et al*., 2005; *Levin et al*., 2005]. The morphotectonic expression of this impingement is the primary topic of this paper.

[3] Late Cenozoic tectonics of the Kamchatsky Peninsula has been previously investigated [*Fedorenko*, 1965; *Kozhurin*, 1985; *Gaedicke et al*., 2000; *Freitag et al*., 2001; *Kozhurin*, 2007; *Baranov et al*., 2010; *Pflanz et al*., 2012], based primarily not only on mapping of active faults but also on geomorphology, trenching, and thermochronology. Historical seismicity has been also analyzed (compilations in *Geist and Scholl* [1994] and *Mackey et al*. [2010]), as well as Holocene tsunami history [*Bourgeois et al*., 2006]. Another indicator of the peninsula's active tectonics is

[1]Department of Geosciences, Normandie University, Caen, France.
[2]UCBN, Caen, France.
[3]CNRS, UMR 6143, Caen, France.
[4]Université de Brest, UMR 6538/CNRS Domaines océaniques, Plouzané, France.
[5]Institute of Volcanology and Seismology, FED, RAS, Petropavlovsk-Kamchatsky, Russia.
[6]Department of Earth and Space Sciences, University of Washington, Seattle, Washington, USA.
[7]Université de Toulouse, UPS (OMP), LMTG, Toulouse, France.
[8]IRD, LMTG, Toulouse, France.
[9]CNRS, LMTG, Toulouse, France.

Corresponding author: K. Pedoja, Normandie University, 2-4 Rue des Tilleuls, 14000 Caen, France. (kevin.pedoja@unicaen.fr)

0278-7407/13/10.1002/tect.20051

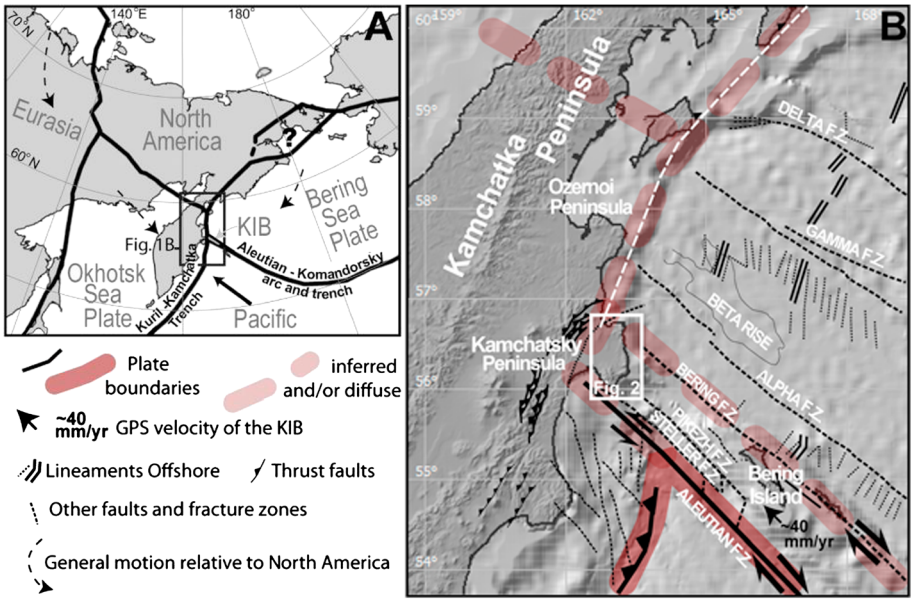

Figure 1. Tectonic setting of central eastern Kamchatka. (a) Location and plate tectonics: Bering block as in *Mackey et al*. [1997], Okhotsk block as in *Gordeev et al*. [2001], and KIB (Komandorsky Island block) as in *McElfresh et al*. [2002]. Arrows show suggested motion of plates relative to fixed North America. (b) Tectonic setting detail from Figure 1a, compiled and revised from *Geist and Scholl* [1994], *Gaedicke et al*. [2000], and *Baranov et al*. [2010]. The position of the northern boundary of the Okhotsk Sea plate is not well defined (shown by a broad band); some models place it as far south as the Kamchatsky Peninsula.

present along the coast of the Kamchatsky Peninsula, particularly its eastern part, in the form of Holocene and Pleistocene sequences of uplifted marine terraces. *Pedoja et al*. [2006], through marine terraces analyses, calculated uplift rates for a segment of the Kamchatsky Peninsula coast (~0.15–1 mm/yr), as well as for the Ozernoi Peninsula to the north (Figure 1b). In the current paper, we expand the marine terrace analyses and add a morphotectonic evaluation of the entire Kamchatsky Peninsula. One of our main objectives is to study well-developed Pleistocene coastal sequences in order to determine uplift rates and to analyze their variations. Field-based study is complemented by drainage analyses of the entire Kamchatsky Peninsula, including areas where no coastal sequences are preserved, using digital elevation model (DEM) and satellite images and morphometric methods. These combined analyses are used to quantify drainage evolution, to highlight structures affecting the entire onshore zone, and thereby to refine our knowledge of active tectonics on the whole peninsula. We suggest that the current deformation observed in the peninsula is produced by impingement of the Aleutian-Komandorsky island chain and by dextral motion of its transform plate boundary. The potential continuity of onshore faults with offshore faults associated with this transform plate boundary is then discussed.

2. Geological Background of Plio-Quaternary Geology

2.1. Tectonic Setting

[4] Currently, the Kamchatsky Peninsula is located in the interaction zone between three major plates (Pacific, Eurasia, and North America) and minor plates consisting of the Okhotsk plate at the eastern part of the Eurasian plate [*Gordeev et al*., 2001; *Apel et al*., 2006], the Bering plate at the northwestern part of the North American plate [*Lander et al*., 1996, *Mackey et al*., 1997; *Cross and Freymueller*, 2008], and the Komandorsky Island block corresponding to the western part of the Aleutian-Komandorsky arc between the North American plate and the Pacific plate [*McElfresh et al*., 2002] (Figure 1).

[5] The Cenozoic structure of the western Aleutian-Komandorsky arc is defined by an active fault zone interpreted as a transform plate boundary with a dextral strike-slip increasing westward along the fault zone [*Geist and Scholl*, 1994; *Cross and Freymueller*, 2008]. As measured by GPS, the short-term movement of the Komandorsky Island block is northwestward (relative to North America) at the rate of ~40 mm/yr [*Gordeev et al*., 2001] (Figure 1b).

[6] The present-day subduction of the Pacific plate along the Kuril-Kamchatka trench has its northern termination along the central part of the eastern coast of Kamchatka. Southeast of the Kamchatsky Peninsula, the trench interacts with the Komandorsky dextral transform plate boundary (Figure 1). This Komandorsky-Kamchatka junction at the Kamchatsky Peninsula can be identified as an area of active arc-continent (or "arc-arc") collision. Indeed, the entire Kamchatka Peninsula was formed during the Cenozoic by several arc accretions against the Kamchatka margin, the latest collision forming the Kamchatsky Peninsula [*Bakhteev et al*., 1992; *Kimura*, 1996; see *Scholl*, 2007 for review]. The timing and details of the impingement and the interactions among theses arcs are an area of active study [*Seliverstov*, 1983; *Geist and Scholl*, 1994; *Lander et al*., 1996; *Mackey et al*., 1997; *Seliverstov*, 1998; *Gaedicke et al*., 2000; *Konstantinovskaia*, 2000, 2001; *Freitag et al*., 2001; *McElfresh et al*., 2002; *Kozhurin*, 2004, 2007; *Solov'ev et al*., 2004; *Levin et al*., 2005; *Steblov and Kogan*, 2005; *Alexeiev*

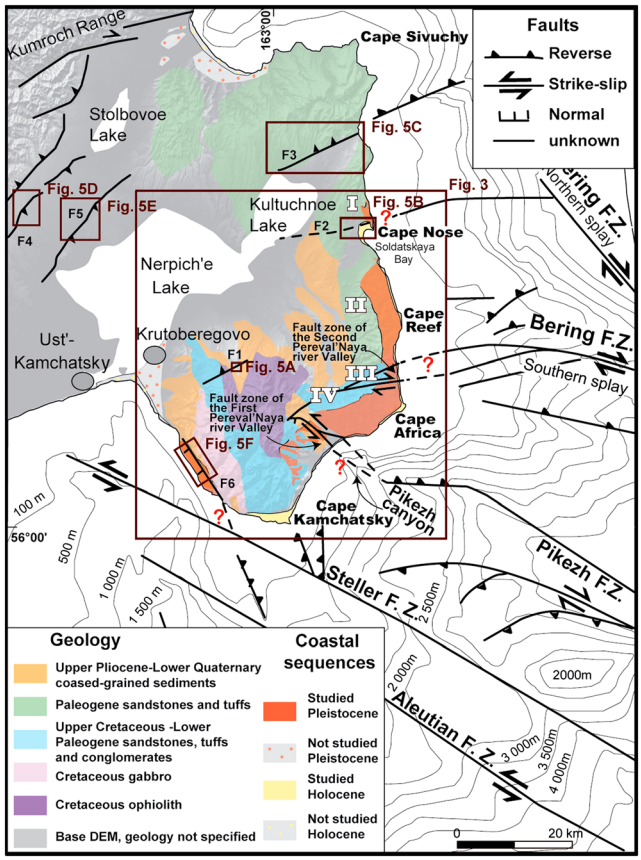

Figure 2. Geologic and tectonic setting of the Kamchatsky Peninsula showing the location of coastal sequences (i.e., marine terraces, beach ridges, and wave-built terraces). Geologic and tectonic setting redrawn from previous authors (see text for references) and is subject to interpretation; question marks indicate tenuous, suggested onshore connections proposed by *Freitag et al*. [2001]. The faults are mapped from the literature, from our field work, and from our observations on DEM and aerial images.

et al., 2006; *Lees et al*., 2007; *Scholl*, 2007; *Cross and Freymueller*, 2008; *Seliverstov*, 2009; *Shapiro and Solov'ev*, 2009; *Mackey et al*., 2010; *Baranov et al*., 2010]. However, the boundaries between these ancient arcs are currently inactive; therefore, we considered the (continental-scale) Kamchatka Peninsula as continental in nature.

[7] The relationships between mapped, offshore faults associated with the Aleutian-Komandorsky plate boundary and mapped, onshore faults on the Kamchatsky Peninsula are poorly constrained because of the data gap under the continental shelf (Figure 2, red question marks). Moreover, the origin and scale of data obtained offshore and onshore are quite different. Offshore of the Kamchatsky Peninsula, on the western tip of the Aleutian-Komandorsky arc, the seafloor exhibits a complicated structure comprising a number of fracture zones represented by dextral strike-slip with thrust components (Figure 2). The Steller and Aleutian fault zones (Figure 2) as mapped by *Gaedicke et al*. [2000] (based on earlier studies) define the southern boundary of the Kamchatsky Peninsula and correspond to the dextral limit of the Aleutian-Komandorsky arc to the south. Relative motion on this fault zone becomes sinistral westward of the Kuril-Kamchatka trench. The northern boundary of the arc is associated with the dextral Bering fault zone (Figure 1). Onshore, on the Kamchatsky Peninsula, major faults have been also recognized [*Kozhurin*, 1985, 2004, 2007; *Bakhteev et al*., 1992; *Gaedicke et al*., 2000, *Freitag et al*., 2001, *McElfresh et al*., 2002] (Figure 2). *Gaedicke et al*. [2000] presented maps showing the faults offshore and onshore as connected (Figure 2), whereas *Kozhurin* [2007] questioned these connections. Better understanding of the active regional fault system is necessary for correct interpretation of the impingement of the Aleutian-Komandorsky arc (more specifically, the Komandorsky Island block) on Kamchatka.

[8] Three models for the Aleutian-Komandorsky-Kamchatka interaction have been proposed: (1) Distributed shear across the Aleutian-Komandorsky arc results in westward movement and subsequent collision (or stuffed subduction) with Kamchatka at the Kamchatsky Peninsula [e.g., *Gaedicke et al*., 2000]; (2) the distributed shear is taken up by block clockwise rotations, with strike-slip and normal faulting [*Kozhurin*, 2007]; and (3) the Komandorsky Island block is only apparently moving to the west as measured by transient GPS; accumulated strain would be released in earthquakes, snapping the islands back to earlier positions [*Steblov and Kogan*, 2005]; this latter interpretation represents a model where the Komandorsky Island block and the Bering plate remain part of the North America plate.

2.2. Geology

[9] The Kamchatsky Peninsula (Figure 2) is composed of a broad variety of rocks and sediments ranging in age from Early Cretaceous to Holocene [*Tsukanov*, 1991], of which we focus on sequences of later Pleistocene marine terraces and present relevant data back to the early Pleistocene. The Cretaceous to lower Pleistocene formations are locally overlain with angular discordance by middle and upper Pleistocene and also Holocene soil-tephra sequences [*Pevzner et al*., 1997; *Ponomorova et al*., 2007] and shallow-marine sediments. The upper Pliocene to lower Quaternary Olkhovskaya Formation caps large portions of the peninsula and is characterized by coarse-grained, semiconsolidated, marine sediments [*Basilyan and Bylinskaya*, 1997]. The maximum uplift (from below sea level) for this formation is estimated to be 1500–2000 m on the southeastern Kamchatsky Peninsula, giving a mean uplift rate of 1.0–1.3 mm/yr, which decreases to zero toward the west, near Ust' Kamchatsk (Figure 2) [*Basilyan and Bylinskaya*, 1997]. Involvement of the Plio-Pleistocene Olkhovskaya Formation in mélange formation gives additional evidence for the active tectonics occurring on the Kamchatsky Peninsula [*Bakhteev et al*., 1993].

[10] The coast of the Kamchatsky Peninsula in many places looks like a huge staircase, which consists of Pleistocene and Holocene terraces, as also observed in other very active parts of the Pacific Rim (e.g., Mahia Peninsula in New Zealand) [*Berryman*, 1993a, 1993b]. The shape of terrace cross-sectional profiles depends essentially on the direction and character of relative sea level change driven by local crustal deformation and by longer-term, glacioeustatic trends imposed on local tectonic trends [*Lajoie*, 1986]. The "stairs" of Pleistocene terraces are typically separated by scarps from 10 to 100 m high, and a sequence of Pleistocene marine

terraces, (including latest of Pliocene in certain areas [see *Pedoja et al*., 2011, Figure 2A]) is interpreted as the geomorphic expression of repeated glacioeustatic high sea level stands superimposed on a rising coastline. The stairs of Holocene terraces are commonly separated by scarps from 0.5 m to several meters high, and such features are evidence of abrupt changes of relative sea level during the Holocene (as in *Ota and Yamaguchi* [2004]). Details of the Holocene terrace record are the subject of another study by our group [*Pinegina et al*., 2010, 2013] and will be compared herein with Pleistocene data.

2.3. Previous Work on Marine Terrace Sequences and Drainage Patterns

[11] Pleistocene marine terrace sequences of the eastern part of the Kamchatsky Peninsula have been previously partially and briefly described or mentioned [*Erlikh et al*., 1974; *Fedorenko*, 1965; *Kozhurin*, 1985; *Pedoja et al*., 2006; *Baranov et al*., 2010; *Pinegina et al*., 2010; *Pflanz et al*., 2012]. In the north of the central part of the eastern Kamchatsky Peninsula, *Pedoja et al*. [2006] mapped five Pleistocene marine terraces along more than 20 km of the coastline. Following standard practice [*Lajoie*, 1986; *Johnson and Libbey*, 1997], the prominent T1 marine terrace was correlated with interglacial Marine Isotopic Stage (MIS) 5 (i.e., last interglacial 85–130 kyr); the shoreline of this terrace was tied to MIS 5e (circa 120 kyr). This correlation yielded long-term uplift rates ranging from 0.10 ± 0.07 mm/yr (0.1 m/kyr) to 1.12 ± 0.20 mm/yr (1 m/kyr), rates comparable to those determined by the same method in other areas of the Western Pacific Rim [*Ota and Yamaguchi*, 2004]. For carving of the T2 terrace, *Pedoja et al*. [2006] favored for most transects a correlation with MIS 9 (circa 330 kyr) rather than MIS 7 (circa 220 kyr). As other authors had [e.g., *Zazo*, 1999], (see http://asterweb.jpl.nasa.gov/gdem.asp), *Pedoja et al*. [2006] postulated that because MIS 7 was probably weaker than MIS 5 or MIS 9, the terraces correlated to MIS 7 were preserved only where uplift rates have been medium to high [see *Pedoja et al*., 2011]. Further field observation and synthesis [*Pedoja et al*., 2011] have led to reconsideration of this postulate, as detailed below. Recently, *Pflanz et al*. [2012] have dated via optically stimulated luminescence deposits from a marine terrace located south of Krutoberegovo (see the unstudied Pleistocene coastal sequence in Figure 2). The deposits (taken at 66 ± 0.5 m) yielded an age of 111.8 ± 10.5 kyr that could suggest a correlation either to MIS 5c (105 kyr) or MIS 5e (120 kyr). In any case, the resulting uplift rate (0.8 ± 0.1 mm/yr, given by *Pflanz et al*. [2012]) is within the range of coastal uplift rates we have calculated [*Pedoja et al*., 2006; this study].

[12] Interactions between fault activity and drainage patterns have to date been studied primarily on the coastal fringe of the peninsula [*Gaedicke et al*., 2000; *Freitag et al*., 2001; *Kozhurin*, 2007, *Baranov et al*., 2010; *Pflanz et al*., 2012], in particular along the first and second Pereval'naya River valleys (Figure 2). Examining offset of Quaternary alluvial deposits and striations affecting Pliocene formations, *Freitag et al*. [2001] and *Gaedicke et al*. [2000] interpreted the faults exposed along the first Pereval'naya River valley as the onshore trace of the dextral Pikezh fracture zone (Figure 2). Instead, *Kozhurin* [2007] considered the entire fault of the first Pereval'naya River to be largely normal according to SW facing scarp affecting alluvial deposits. *Kozhurin* [2007] also indicated a small sinistral component, also observed by *Baranov et al*. [2010], showing left-lateral stream offsets of around 30–40 m. Along the main fault of the second Pereval'naya River valley (Figure 2), another fault zone affects Quaternary alluvial deposits and the current drainage. According to reverse offsets of alluvial deposits and marine terraces, *Freitag et al*. [2001], *Gaedicke et al*. [2000], and *Pflanz et al*. [2012] assigned to this fault zone a reverse motion. *Kozhurin* [2007] interpreted the kinematics of the same fault zone to be right lateral, with an estimated Quaternary slip rate of 4 mm/yr, based on offsets of dated alluvial terraces.

3. Approach and Methods

[13] In this section, we first present our estimation of coastal uplift rates based on elevation of shoreline angles of marine terrace sequences on the southeastern part of the peninsula. Then we present the drainage analysis that we performed, first on the studied marine terrace area and then through DEM observations, extended to other parts of the peninsula where coastal sequences are neither present nor preserved or were not visited.

3.1. Coastal Uplift Rates

[14] The interpretation of marine terraces as formed during separated highstands of interglacial stages correlated to marine oxygen isotopic stages and/or substages (MIS or MISS) [*James et al*., 1971; *Chappell*, 1974; *Bull*, 1985; *Ota*, 1986] is now widely applied to Pleistocene terrace sequences. Each marine terrace is characterized by a shoreline angle, i.e., the angle between the fossil marine abrasion platform and the associated paleo–sea cliff. This geomorphic indicator represents the maximum extension of a transgression and, therefore, a highstand in the former sea level. Vertical displacement of the shoreline relative to the age of the associated interglacial stage yields a mean uplift rate. The classic equation [e.g., *Lajoie*, 1986] for calculating vertical motion rate V is

$$V = (E - e)/A,$$

where E is the current elevation of the paleo–shoreline relative to the current local sea level, A is the age of MIS 5e, and e is the correction for eustasy (i.e., the altitude of the paleo–sea level stand relative to the modern one). In the present study, we calculate the mean displacement rate since MIS 5e using a simpler, yet more conservative method [*Pedoja et al*., 2011]. We do not account for any a priori eustatic correction e and simply calculate $V = E/A$. In fact, estimates on sea level variations during MIS 5e (with respect to today's datum) are principally based on coastal indicators found on platforms formerly considered stable, an assumption revealed to be uncertain (see discussion in *Pedoja et al*. [2011]).

3.2. Altitude Measurements of Pleistocene Shoreline Angles

[15] Altitudes of Pleistocene shoreline angles were measured with digital altimeters calibrated to the last high tide mark observed on the shore. The local mean sea level was determined from tide tables. We assume that the uplifted terraces were formed under tide conditions similar to the

present, with a tide range of less than 2 m. With the same altimeter, we estimated barometric drift and made a calibration on the reference point after the altitude measurements. The major error on the measured shoreline angle altitude comes from preservation quality and elevation of the shoreline angle. Disturbance could come, for example, from erosion of sea cliffs or cover of terraces by colluvium and glacial deposits. In most cases in this field area, only the morphology of the terrace is preserved; marine deposits are either lacking or buried.

[16] The shoreline angles of Kamchatsky Peninsula terraces are commonly covered by about 5 m of colluvium or glacial deposits, and the oldest (uppermost) ones are barely observable, whereas the two or three lower ones can be seen easily in the landscape. In all sequences, the best preserved terrace is the lowest one, which is tentatively correlated to MIS 5e. Individual patterns of deformation in each area, since the period of time represented by the four Pleistocene marine terraces (T1 = MIS 5, Substage 5e; T2 = MIS 7 or 9; T3 = MIS 9 or 11; T4 = MIS 11 or older), were previously established along the northern part of the central eastern coast of the Kamchatsky Peninsula [*Pedoja et al*., 2006].

3.3. Evaluation of Active Tectonics From Topography and Drainage Patterns

[17] Physiographically, the Kamchatsky Peninsula combines several isolated mountainous massifs adjacent to a lowland in the west central part of the peninsula, with the large lakes Stolbovoe, Nerpich'e, and Kultuchnoe (Figure 2). We analyzed Quaternary geomorphic markers (alluvial terraces, fans) and the drainage patterns incising this relief to help in the identification of active tectonics (as in *Merritts and Vincent* [1989], *Burbank and Anderson* [2001], *Keller and Pinter* [2002], and *Regard et al*. [2009]). First, topographic profiles were produced along geomorphic features affected by inferred faults in order to identify vertical tectonic offset. Second, a qualitative analysis of the drainage network geometry was realized to identify active zones in terms of relative vertical motion and tilting [e.g., *Delcaillau et al*., 1998]. Finally, three geomorphic indices were extracted from the topography: (1) asymmetry of watersheds [*Cox*, 1994], (2) shape of stream long profiles [e.g., *Hack*, 1973; *Hare and Gardner*, 1985; *Molin et al*., 2004], and (3) hypsometric integral [*Stralher*, 1952; *Hurtrez et al*., 1999]. In this study, the drainage network was automatically derived from the 20 m horizontal resolution DEM Advanced Spaceborne Thermal Emission and Reflection Radiometer (ASTER). For 21 basins and associated major streams over the peninsula, the longitudinal stream profile and the hypsometric integral were calculated from the DEM ASTER analysis with RiverTools software (http://www.rivix.com/).

4. Results

4.1. Pleistocene (and Holocene) Marine Terrace Sequences

[18] Morphologically, the southeastern coast of the Kamchatsky Peninsula is characterized by two distinct marine terrace sequences: the Holocene sequence and, topographically above it, the Pleistocene one (Figures 3 and 4). The Pleistocene sequence of marine terraces includes a maximum total of five "first-order" marine terraces. We call first-order terraces the marine terraces whose width is >500 m with a well-defined shoreline angle (base of a high paleo–sea cliff). First-order terraces can be compounds of various "second-order" terraces. For example, in some places, T1 is composed of at least two distinct platforms (T1′ and T1″) separated by a small scarp (<20 m elevation difference), barely noticeable in the landscape (see, for example, Figure 4d, transect 4). In the case of the marine terrace T1 of transect 4 (Figure 4d), we interpret these terraces to be the result of sea level stability during second-order highstands (Substage 5a or 5c) of the last interglacial, MIS 5. Such small terraces are probably also present on older Pleistocene marine terraces of the sequence, but they are barely noticeable because of erosion, particularly glacial erosion, as well as deposition, processes that have been active and have partially buried or eroded the intermediary shoreline angles.

[19] We divide the southeastern coast of the Kamchatsky Peninsula into four different zones (named I, II, III, and IV in Figures 2, 3, 4c, and 4d) characterized by their deformation pattern, as follows.

4.1.1. Cape Nose Block (Zone I)

[20] The Cape Nose block is bounded to the north by vertical cliffs and to the south by Soldatskaya Bay (Figure 2). The southern boundary is also marked by a fault (Figures 2 and 5b, F2). In Zone I, the marine terrace sequence reaches 90 ± 5 m in altitude. The sequence is composed of at least three Pleistocene marine terraces overlooking the Holocene sequence. Three altitudinal transects of the Pleistocene terraces were performed around Cape Nose (Figure 4d). Maximum altitudes of the shoreline angles of T1, T2, and T3 were measured on the northernmost transect (Figures 3 and 4, transect 1) at the following altitudes: 25 ± 3 m (T1), 60 ± 5 m (T2), and 90 ± 5 m (T3). Minimum altitudes of the shoreline angles of T1, T2, and T3 were measured on the southernmost transect (Figures 3 and 4, transect 3) at the following altitudes: 20 ± 3 m (T1) and 55 ± 5 m (T2). Given the error range, it is not possible to determine conclusively whether there is a tilting of the sequence toward the south or an offset produced by fault motion (Figure 5b, fault F2). The T1 marine terrace has been correlated with the last interglacial maximum (MIS 5 Substage 5e) [*Pedoja et al*., 2006].

4.1.2. Cape Reef Block (Zone II)

[21] From the southern side of Soldatskaya Bay southward to Cape Reef (Figures 2, 3, and 4d), over 15 km, the Pleistocene marine terrace sequence fringes the coast on a faulted and tilted block that we name the Cape Reef block. The altitude of the lowest Pleistocene marine terrace (T1) rises from 55 ± 3 m in the north (Figure 4d, transect 4) to 180 ± 15 m in the south (Cape Reef; Figure 4c, transect 8). This terrace is correlated with the last interglacial maximum (MIS 5 Substage 5e) [*Pedoja et al*., 2006]. Walking the beaches of this zone, and during helicopter flight, and on imagery (air photo, Landsat, etc.), we observed the morphological continuity of the sequence. Therefore, relative tectonic motion can be inferred from the difference in altitude of the same terrace. That is, the southern part of Zone II has experienced a 3 times stronger uplift than the northern part. The correlation of T1 to MIS 5e leads us to propose mean uplift rates ranging from 0.46 ± 0.07 mm/yr (north) to 1.49 ± 0.22 mm/yr (south) for the late Pleistocene (Figure 3 and Table 1).

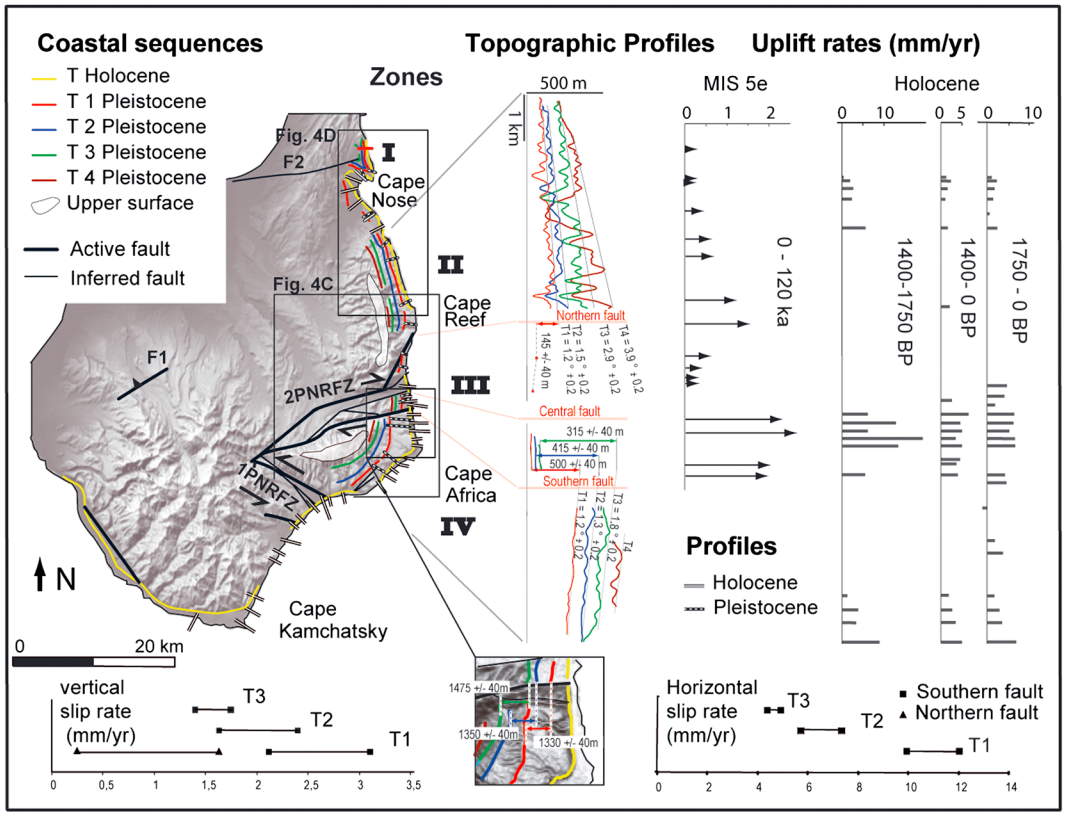

Figure 3. Uplift of the east central coast of the Kamchatsky Peninsula and analysis of faulting and tilting affecting the Pleistocene marine terrace sequence. Mapped outline and topographic profile of Pleistocene and Holocene shoreline angles, based on this work and *Pedoja et al*. [2006] (northern zone, Pleistocene). Holocene coastal uplift rates are from *Pinegina et al*. [2010, 2013]. All values (uplift, slip rates) are in millimeters per year or the equivalent meters per kiloyear. Different time intervals show similar trends but different rates, as discussed in *Pinegina et al*. [2010]. Topographic profiles, vertical offsets, and tilting angles for Pleistocene marine terraces T1–T4, from DEM and from altitude transects. These profiles are oriented parallel to their mapped images, above, but the horizontal scale is slightly different (e.g., there is a break in the horizontal scale, below). Faults are discussed in the text. (inset) From displaced terrace morphology, analysis of horizontal slip rates along faults between Zones III and IV, north of Cape Africa, and vertical slip rates along these same fault zones and the fault south of Cape Reef.

[22] Three older marine terraces (T2, T3, and T4) and an upper planation surface (Figures 3 and 4) overlook the young Pleistocene marine terrace (T1) as well as the Holocene sequence. We produced NNW-SSE trending topographic profiles along each shoreline angle of the marine terraces in order to observe potential tilting (Figure 3). The strike of each geomorphic marker (i.e., the shoreline of each marine terrace) shows a tilting up toward the south, with the tilt angle for progressively higher terraces increasing in relation with age. The oldest mapped marine terrace (T4) is tilted $3.9 \pm 0.2°$, a tilt 3 times higher than that of T1 ($1.2 \pm 0.2°$) (Figure 3 and Table 2). This increase of northward tilt with age is consistent with a tilt induced by continuing vertical motion along the NE-SW trending northern fault of the second Pereval'naya River fault zone (2PNRFZ), at the southern boundary of Zone II (Figure 3).

4.1.3. The Second Pereval'naya River Block (Zone III)

[23] Zone III (Figures 3 and 4c) essentially comprises the second Pereval'naya River valley affected by the fault zone bearing the name of the river (2PNRFZ). In Zone III, the sea cliffs are reduced (heights ranging from 20 to 50 m), and the T1 marine terrace (Figure 4c) is found at an altitude distinctly lower than to the north (Zone II) and to the south (Zone IV). In Zone III, unlike Zones II and IV, T4 and the upper surface are not present in the landscape, and the T3 paleo–sea cliff corresponds to the highest point of the area (Figure 4c). We conclude that this zone probably emerged above sea level after the uplift and emergence of the blocks to the north and to the south (Figure 4c, Zones II and IV). In Zone III, tentative correlation of T1 to the last interglacial maximum (MIS 5e) leads us to propose mean uplift rates ranging from 0.54 ± 0.08 to 0.27 ± 0.04 mm/yr for the late Pleistocene.

[24] After a sharp shift in altitude of T1 at the boundary between Zones II and III (180 ± 15–65 ± 5 m), T1's altitude in Zone III decreases to the south more gradually (65 ± 5 to 28–32 ± 4 m) on transects 9–12 (Figures 3 and 4c). South of the Zone III boundary, T1 is significantly higher (330 ± 20 m) in Zone IV (Figures 3 and 4c). The vertical offsets of T1 on the northern (145 ± 40 m) and on the southern (315 ± 40 m) boundaries of Zone III are most likely associated with vertical displacement along the southern and northern faults of

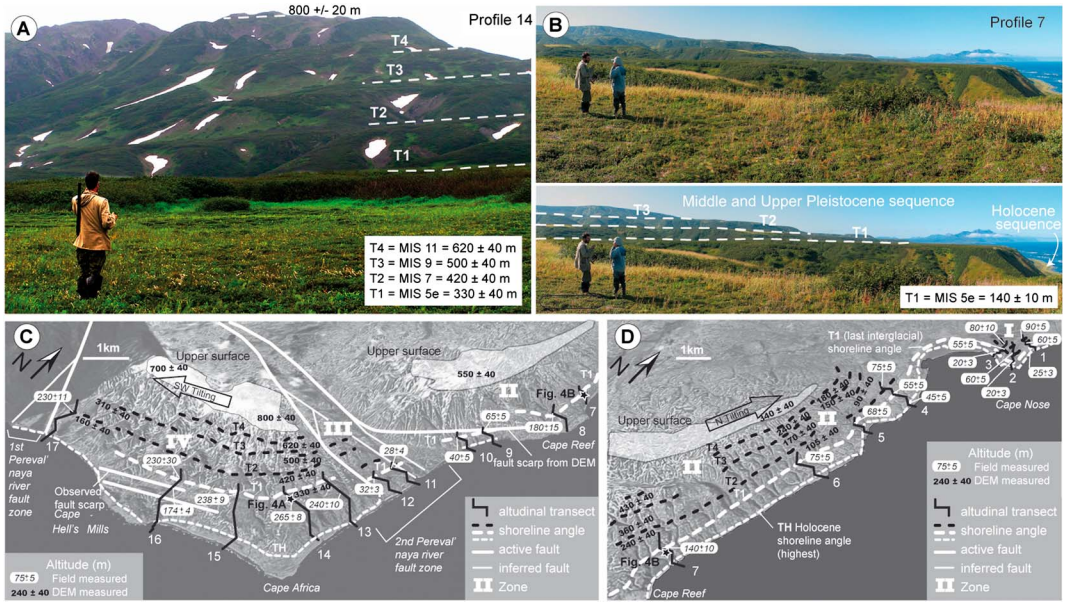

Figure 4. Morphologic expression of the middle and upper Pleistocene marine terraces. (a) Interpreted photo of Mount Africa (profile 14). (b) Interpreted photo of Cape Reef marine terrace. (c and d) Three-dimensional oblique views (Google Earth image) of the Holocene and Pleistocene coastal sequences. Elevations shown in italics are based on field measurements along numbered transects; elevations in bold black are from DEM analysis. Figure 4c shows the eastern coast from Cape Nose to Cape Reef. Figure 4d shows the eastern coast from south of Cape Reef around Cape Africa. Scale and orientation of both images are about the same.

the 2PNRFZ (Figure 3). The higher vertical component of displacement along the southern fault also affects the older marine terraces: T2 (offset 415 ± 40 m) and T3 (offset 500 ± 40 m), vertical offsets increasing in agreement with marine terrace age.

[25] The marine terraces between Zones III and IV also show right-lateral offsets at the southern boundary of the 2PNRFZ, in agreement with the right strike-slip fault kinematics assigned by *Kozhurin* [2007]. The horizontal offsets are 1330 ± 40, 1350 ± 40, and 1475 ± 40 m of the shoreline angles of T1, T2, and T3, respectively, thus increasing with offset marine terrace age. These offsets plus the vertical motion imply an oblique dextral motion of the fault zone. As the fault dip is unknown, we cannot determine if it is transpressive or transtensive kinematics.

[26] We estimate vertical and horizontal slip rates on the northern and southern faults of the 2PNRFZ of Zone III according to the location, altitude, and age of marine terraces north and south of those faults. According to the T1 vertical offset, our age assignments (Table 2) lead to vertical slip rates ranging from 2.1 to 3.1 mm/yr along the northern fault of the 2PNRFZ and from 0.8 to 1.6 mm/yr for the southern fault of the 2PNRFZ (Figure 3). On the northern fault, older vertical offset rates can be calculated according to T2 as from 1.6 to 2.3 mm/yr and according to T3 from 1.4 to 1.7 mm/yr. It seems that vertical slip rate decreases with age, a tendency also shown by horizontal slip rates estimated on the southern fault of the 2PNRFZ (Figure 3), where the T1 offset yields horizontal slip rates from 9.9 to 12 mm/yr, T2 from 5.7 to 7.3 mm/yr, and T3 from 4.3 to 4.9 mm/yr. This decrease could be due to heterogeneous fault activity during a relatively short-period (~330 year) cyclic fault activity or a decrease of the convergence rate of the Komandorsky Island block affecting onshore fault activity.

4.1.4. Cape Africa Block (Zone IV)

[27] On Cape Africa (Zone IV), between the second and first Pereval'naya River valleys, a high Holocene sequence (up to >30 m above mean sea level) lies at the foot of a high Pleistocene sequence (Figures 3 and 4), with the T3 and T4 terraces and the upper surface well preserved above the younger terraces (Figures 4a and 4c). In Zone IV, the Pleistocene marine terrace sequence reaches its maximum altitude on the Kamchatsky Peninsula: 330 ± 20 m for T1, 420 ± 40 m for T2, 500 ± 40 m for T3, and 620 ± 40 m for T4 plus an upper surface at 800 ± 20 m (Figures 4a and 4c). Correlation of T1 to MIS 5e yields mean uplift rates ranging from 1.91 ± 0.37 to 2.73 ± 0.34 mm/yr for the late Pleistocene.

[28] In Zone IV, the Pleistocene marine terraces and the modern abrasion platform are wide, separated by a narrow Holocene accumulative sequence [*Pinegina et al.*, 2010, 2013]. The T1 terrace is wider than 1.5 km and is probably compound on Cape Africa. We observed at least two "steps" (scarps) in the T1 surface (Figure 4c). Because the map trace of these scarps is straight and nonconforming to the modern shoreline, we tentatively interpret these scarps as NW-SE trending faults (Figure 4c), but these scarps might be superposed, former intermediate shorelines. The morphology of this part of the coast is strongly affected by active faulting, as described by other authors [e.g., *Baranov et al.*, 2010].

[29] The sequence of terraces on Cape Africa manifests a southwestward tilt (Figures 3 and 4c). The T3 marine terrace is tilted $1.8 \pm 0.2°$, T2 is tilted $1.3 \pm 0.2°$, and T1 is tilted $1.2 \pm 0.2°$. These tilts are lower than for the marine terraces in the Cape Reef block (Zone II), which has a maximum tilt

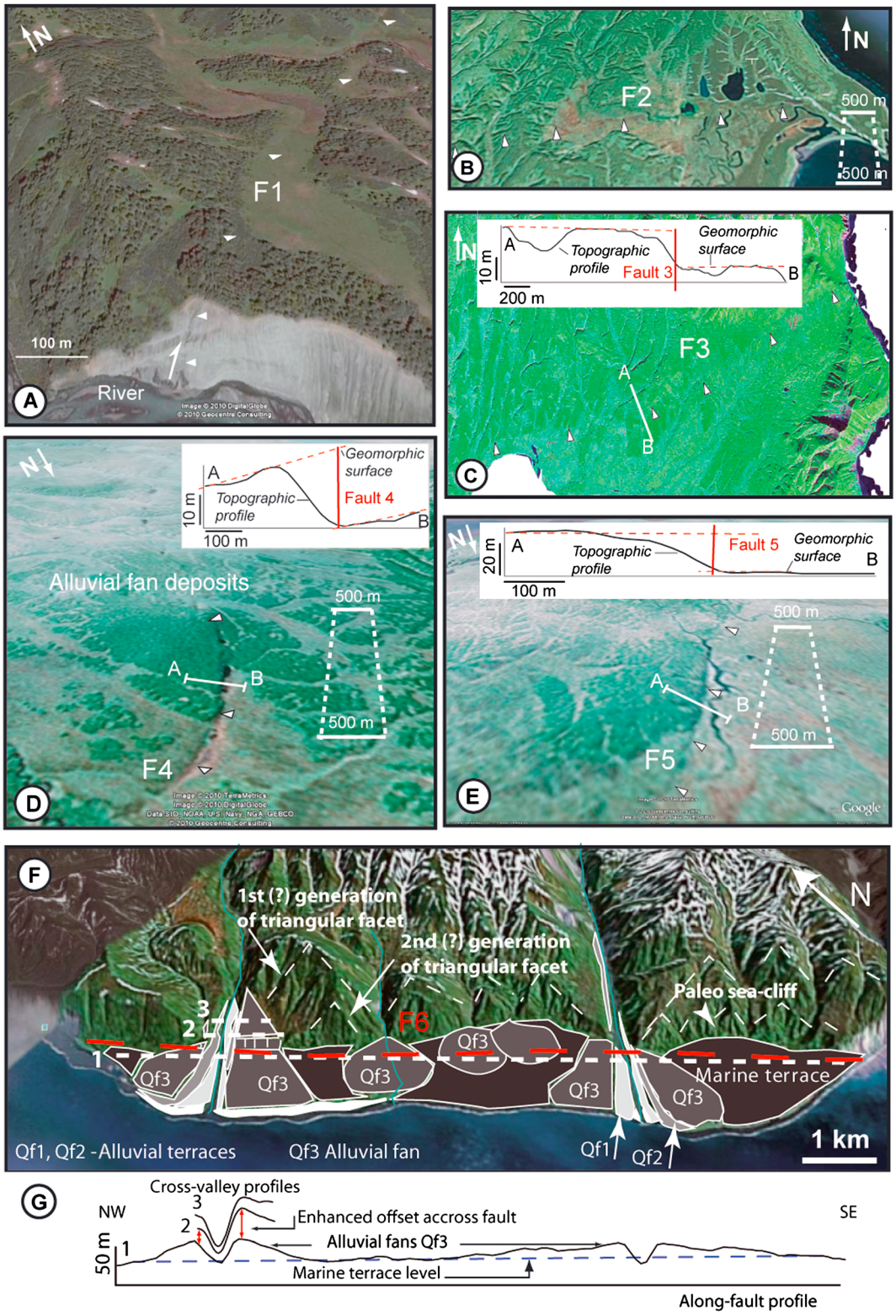

Figure 5. Morphological observations on the Kamchatsky Peninsula. For all the subfigures, see location in Figure 2. (a) Reverse fault (F1) affecting the Olkhovsk deposits as seen on Google Earth. (b) Fault trace of F2 fault revealed by a trellis drainage pattern as observed on Google Earth. (d and e) Fault scarps of F3–F5 as deduced from topographical analysis on DEM (profiles below photos). (f and g) Morphotectonics to the SW from Cape Kamchatsky, focused on fault 6 (see Figure 2 for map location). Figure 5f shows the interpreted zone on a 3-D view Google Earth showing the morphotectonics units; the along-fault topographic profile is shown below, at the same horizontal scale. Figure 5g shows profiles: cross-valley profiles 1–5 show enhanced vertical change across fault 6, and the river thalweg profile shows knickpoints, including one across fault 6.

Table 1. Uplift Rates on the Kamchatsky Peninsula

		T1 = MIS 5e				T2 = MIS 7				T3 = MIS 9				T4 = MIS 11			
Zone	No.	*E* T1	MoE	*U*	MoE	*E* T2	MoE	*U*	MoE	*E* T3	MoE	*U*	MoE	*E* T4	MoE	*U*	MoE
I	1	25	3	0.21	0.04	60	5	0.29	0.05	90	5	0.28	0.02				
	2	20	3	0.17	0.04	60	5	0.29	0.05	80	10	0.25	0.04				
	3	20	3	0.17	0.04	55	5	0.27	0.05								
II	4	55	5	0.46	0.07	75	5	0.36	0.06								
	5	68	5	0.56	0.08	90	40	0.45	0.23	150	40	0.47	0.14	180	40	0.43	0.12
	6	75	5	0.62	0.08	105	40	0.52	0.24	170	40	0.54	0.14	240	40	0.58	0.12
	7	140	10	1.16	0.16	240	40	1.17	0.30	360	40	1.13	0.16				
	8	180	15	1.49	0.22	230	40	1.12	0.30	390	40	1.22	0.16	550	40	1.32	0.16
III	9	65	5	0.54	0.08												
	10	40	5	0.33	0.06												
	11	28	4	0.23	0.05	50	20	0.25	0.12	95	40	0.30	0.13				
	12	32	3	0.27	0.04	60	20	0.30	0.12	100	40	0.32	0.13				
IV	13	290	20	2.40	0.32												
	14	330	20	2.73	0.34	420	40	2.04	0.38	500	40	1.57	0.17	620	40	1.48	0.17
	15	238	9	1.96	0.20												
	16	230	30	1.9	0.37												
	17					230	11	0.72	0.06	310	40	0.74	0.13				

No.: transect number; *E* T1, T2, T3, T4: elevation T1, T2, T3, T4; MoE: margin of error; *U* = uplift rate; T1 = Mis 5e (7, 9, or 11): chronostratigraphical interpretation, which means that the shoreline angle of T1 (T2, T3, or T4) has been correlated to a highstand associated with the Marine Isotopic Stage (or Substage) 5e (7, 9, or 11). We considered ages of 122 ± 8, 210 ± 20, 320 ± 10, and 420 ± 20 kyr for MIS 5e, 7, 9, and 11, respectively (see text for details).

of $3.9 \pm 0.2°$ (for T4; Figure 3 and Table 2). The southwestward tilt of Zone IV appears to be accommodated by differential slip on faults along the E-W trend of the 2PNRFZ and the NW-SE trend of the 1PNRFZ located in the first Pereval'naya River valley, which bounds the Cape Africa block. Vertical motion along the 1PNRFZ south of the Cape Africa block (Figure 3) would compensate the tilt produced by vertical motion along the 2PNRFZ. However, the southwestward tilt is maintained, suggesting a larger vertical slip rate of the 2PNRFZ than the 1PNRFZ. This tilting is perpendicular to the southeastward tilting affecting the same geomorphic features described by *Fedorenko* [1965] and *Kozhurin* [1985], who associated this tilting with a NE-SW trending folding due to the interaction between Cape Africa and the Komandorsky Island block. The southwestward tilting we have described is more consistent with a combination of faulting between the 1PNRFZ and the 2PNRFZ than with folding.

4.2. Geomorphic Evidence of Active Faults in the Kamchatsky Peninsula

[30] Analyses of satellite images of Landsat and Google Earth associated with topographic measures using ASTER DEM allow us to distinguish geomorphic evidence of (at least) six active faults (F1–F6) in the Kamchatsky Peninsula (Figures 2, 5, and 6).

4.2.1. Faults F1–F5

[31] F1, striking NE-SW and located north of the massif of Cape Africa, was identified using Google Earth navigation (Figures 2 and 5a). An outcrop of upper Pliocene to lower Quaternary deposits on the slope of a large and incised valley shows a vertical offset of beds on the two sides of the fault with an eastern subsiding fault flank (Figure 5a). In the natural cross section of the valley, the dip of the fault is toward the northwest. Thus, the fault appears in this vertical section as a reverse fault with a high-angle dip and a SE vergence (Figure 5a).

[32] F2, located at Cape Nose, is traced westward, where it could constitute the southern linear boundary of Kultuchnoe Lake (Figure 2). This EW striking fault (Figure 5b) imprints the landscape and seems to affect Quaternary deposits along the coast by limiting the prolongation of the Pleistocene sequence of marine terraces to the north (northern boundary of Zone I). However, the displacement mechanisms cannot be determined as no vertical offset was measured and no lateral offset observed. Consequently, this fault is an inferred fault.

[33] F3 is the southern boundary of the massif of Cape Sivuchy (Figures 2 and 5c). This fault was observed by *Gaedicke et al*. [2000], who described it as a south verging reverse fault associated with well-developed drag folds in the footwall. Topographic profile AB in Figure 5c across the fault in Quaternary deposits shows an apparent vertical topographic offset of ~20 m of the northern block uplifted relatively to the southern block, in agreement with the fault kinematics suggested by *Gaedicke et al*. [2000].

[34] F4 and F5 are located in the northeasternmost zone of the Kamchatsky Peninsula in the large alluvial plain (Stolbovskaya depression) northwest of Nerpich'e Lake (Figure 2). Geomorphic analyses show that F4 and F5 affect

Table 2. Vertical Offsets of the Marine Terraces Along the Northern and Southern Boundaries of Zone III and Induced Vertical Slip Rates

Marine Terrace	Age (kyr)	Vertical Offset Between Zones II and III (m)	Vertical Offset Between Zones III and IV (m)	Tilting of Cape Reef Terraces	Tilting of Cape Africa Terraces	Vertical Slip Rate Between Zones III and IV (mm/yr)	Vertical Slip Rate Along the Southern Segment (mm/yr)
T1	122 ± 8	145 ± 40	315 ± 40	$1.2 \pm 0.2°$	$1.2 \pm 0.2°$	2.1–3.1	0.8–1.6
T2	210 ± 20		415 ± 40	$1.5 \pm 0.2°$	$1.3 \pm 0.2°$	1.6–2.3	
T3	330 ± 10		500 ± 40	$2.9 \pm 0.2°$	$1.8 \pm 0.2°$	1.4–1.7	
T4	420 ± 20			$3.9 \pm 0.2°$			

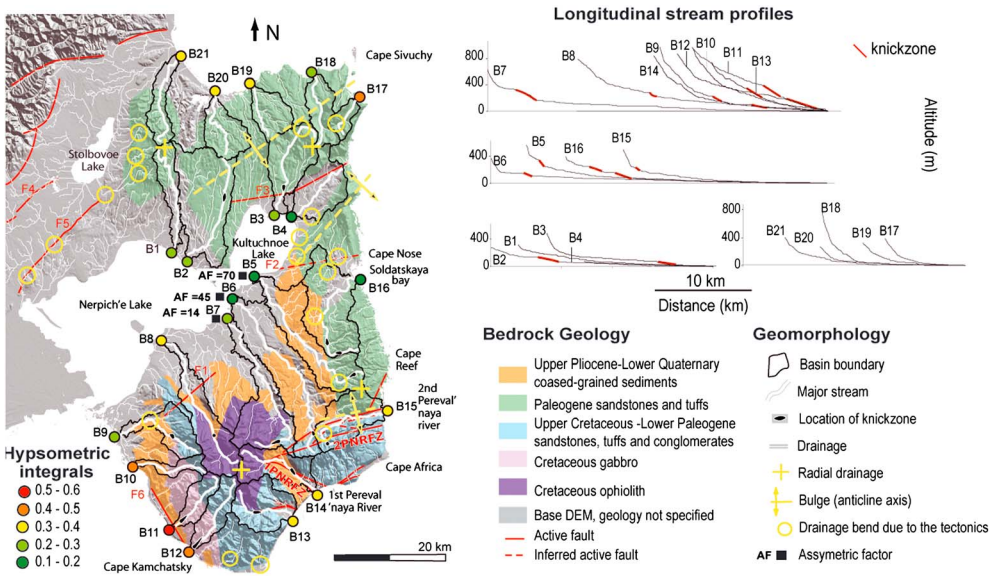

Figure 6. Drainage and morphometry on ASTER DEM. The drainage anomalies for the drainage basins are superimposed on the geological map. Values of hypsometric integrals are shown by color-coded dots for basins B1–B21; see text for discussion. (upper right) Longitudinal profiles were calculated and are plotted for each trunk stream. Stream knickpoints (knickzones) are shown by black ovals on the map and by red lines on the stream profiles.

Quaternary deposits with an apparent vertical motion of about 20–30 m, producing an uplift of the SE flanks of the faults (Figures 5d and 5e). These young topographic offsets control drainage rearrangement (Figure 5e), as indicated by the alignment of ponds along the fault (Figure 5d). The curved fault trace of F4, underlined by the topography and the relative motion of fault walls, leads us to suggest that F4 and F5 are reverse faults with a NW vergence. This interpretation is in agreement with the kinematics of minor faults observed in a trench dug across the fault at the foot of the Kumroch Range (north of F4) and analyzed by *Kozhurin* [2009]. The NW vergence of faults F4 and F5 is opposite to the general SE verging structural grain of the Kumroch Range located to the north of F4. Consequently, the fault activity of F4 and F5 is superposed relative to the uplift of this range.

4.2.2. Fault F6 and Associated Marine Terraces

[35] In the southwestern region of the Kamchatsky Peninsula, a NW-SE trending scarp traces the western coast of Cape Kamchatsky (Figures 2, 5f, and 5g). According to geomorphic indices, we suggest that this scarp is associated with a fault (F6). The inferred fault F6 is parallel to the fault zone along the 1PNRFZ located 20 km eastward [*Gaedicke et al*., 2000; *Freitag et al*., 2001; *Kozhurin*, 2007]. The two faults mark the boundaries of the massif of Cape Kamchatsky (Figures 5f and 5g). Along the coast, the inferred fault F6 seems to control the development of a sequence of two marine terraces (Figure 5f) above the Holocene one and to affect Quaternary alluvial fans (Figure 5f, Qf3).

[36] We did not have the occasion to study this marine terrace sequence in the same detail as those on the eastern coast. On the easternmost part of the sequence, we observed uplifted shallow-marine coastal deposits, including articulated valves of *Chione* sp, *Tagelus* sp, and *Polinices* sp. The deposit containing this fauna lies unconformably above a fluviomarine sequence. The altitude of the shallow-marine deposits and the distal edge of marine terrace T1 was measured at 37 ± 3 m. East of this zone, the westernmost preserved Holocene terrace sequence along this southern shore (Figure 3) exhibits one of the highest uplift rates measured of all 33 Holocene profiles [*Pinegina et al*., 2013, Profile 23].

[37] Between Cape Kamchatsky and Ust' Kamchatsk, we observed various landforms, including marine terraces, fluvial terraces, alluvial fan deposits, and triangular facets (Figures 5f and 5g). The fault scarp of fault F6 appears to be associated with two generations of triangular facets (Figure 5f), which are typically associated with normal faulting. The two generations of facets suggest a long-lived fault with episodes of activity. The topographic profile AB in Figure 5g shows that the fan deposits, associated with a typical convex shape, cover the upper surface of marine terraces at the level of 30 m. Five DEM-generated cross-stream topographic profiles across the western alluvial fan on both sides of the fault F6 (Figures 5f and 5g) suggest motion along the fault that vertically offsets the fan 20–30 m, with an uplifted block NE of the fault. Associated with the observed triangular facets, this motion implies that F6 is a normal fault dipping to the SW.

4.3. Geomorphic Indices of Recent Tectonics in the Drainage of the Kamchatsky Peninsula

4.3.1. Analysis of the Drainage Network Geometry

[38] Drainage anomalies allow us to characterize an uplifted zone in the northern part of the Kamchatsky Peninsula, north of fault F3 (Figure 6), constituted primarily of Paleogene volcaniclastics and sandstone. This zone forms three bulges from Cape Nose toward Stolbovoe Lake (Figure 6). The two northern ones are associated with radial drainage (Figure 6). The bulge near Cape Sivuchy is

elongated with a NE-SW strike, with its axis corresponding to a drainage divide separating a broadly parallel network pattern on the southern side from a dendritic pattern to the north (Figure 6). The elongated bulge could correspond to an anticline in agreement with a compressional regime indicated by the neighboring south verging reverse fault F3 (fault F3 as in *Gaedicke et al*. [2000]). A tilting of the southern flank of the bulge could explain the high-angle bent drainage near the bulge axis as produced by drainage capture of a northern drainage by a southern drainage associated with retrogressive erosion in response to tilting (Figure 6). The southwestern termination of the bulge coincides with the NW-SE en echelon fault system (Figure 6). The juncture between the NW-SE fault system and F2 corresponds to the boundary between the Nerpich'e and Kultuchnoe Lakes, suggesting a tectonic control of the basin connection.

[39] Another elongated, NE-SW trending uplifted zone is defined north of Soldatskaya Bay (Figures 2 and 6). Tilting associating with this uplift is suggested by a change of strike from SW-NE to E-W, perpendicular to a NE-SW trending anticline of three and two drainages west and east of the bulge axis, respectively (Figure 6). Symmetric tilting of flanks on both sides of the bulge axis supports the anticline hypothesis. This bulge or anticline must be recent as it affects these minor deflected drainages.

[40] The two inferred anticlines between Cape Sivuchy and Cape Nose must create a NE-SW trending synclinal depression between them. This depression guides a major drainage flowing ~12 km toward the southwest to Kultuchnoe Lake. The spring of this drainage is located ~1 km from the sea to the north, and no relief blocks the way of the drainage to the sea (Figure 6). This anomaly must imply that the drainage was forced to flow SW by an uplift near the coast, producing a southwestward inclination in this zone (Figure 6). The spring of the stream is localized in the periclinal termination of the syncline. The lakes of Kultuchnoe and Nerpich'e are aligned in the SW prolongation of this NE-SW trending synclinal axis that may indicate that this structure affects a larger area on the Kamchatsky Peninsula.

[41] In the southern part of the peninsula, three uplifted zones are suggested by a radial drainage. The first one corresponds to the southern part of Cape Reef (Figure 6). It is characterized by tilting of the marine terrace sequence. The second uplifted zone corresponds to the Cape Africa massif and is also in agreement with marine terrace analyses. The third zone of uplift, located in the southern part of the peninsula, west of the first Pereval'naya River, is associated with a radial drainage (Figure 6). This region is characterized by the highest summits on the peninsula at around 1200 m of altitude, comprising Cretaceous ophiolites. This lithology could be less erodible than the nearby younger volcano-sedimentary formations and explain the elevation of the relief. However, the eastern flank is associated with asymmetric drainages that imply titling due to uplift (see below).

[42] As a measure of tilting, we calculated the asymmetric factor (AF) [*Cox*, 1994] of three parallel streams with trunks that flow north in between the two southern uplifting zones (Figure 6). Defined as $AF = 100(Ar/At)$, where Ar is the area of the basin to the right (facing downstream) of the trunk stream, and At is the total area of the drainage basin, the factor AF is sensitive to tilting perpendicular to the trunk-stream trend. A stream that formed and continues to flow in a stable setting has an AF of ~50, whereas values greater or less than 50 may suggest tilt. In our study, the western stream, which drains the western uplifting zone, has an AF of 14; that is, tributaries on the western side of the trunk stream are long compared to those on the east side. This result implies that tectonic tilting is down to the east, in agreement with western uplift. As these streams mostly incise Pliocene conglomerate, the age of the tilting produced by uplift must be younger than Pliocene. The central stream has an AF of 45, and the eastern stream (draining the eastern uplift zone) has an AF of 70. This AF change from west to east from a value <50 to one >50 suggests a tectonic depression in between the uplifting zones.

4.3.2. Longitudinal Stream Profiles

[43] Variations in channel profiles and presence of knickzones depend on gradients in rock uplift rate, occurrence of base level fall, and contrasts in lithology [*Gardner*, 1983; *Whipple and Tucker*, 1999; *Kirby and Whipple*, 2001; *Zaprowski et al*., 2001; *Molin et al*., 2004; *Duvall et al*., 2004; *Bishop et al*., 2005]. A concave-up stream profile indicates that morphodynamic equilibrium has been reached. Most of the channel profiles in this study show a general concave-up shape with local straight or convex reaches/knickzones (Figure 6). These knickzones could be the result of base level drop due to eustatic fall of sea level, in which case the anomaly should be present on all profiles connected to the sea. However, in this study, one third of such streams (Figure 6; B22, B21, B20, B19, B18, B4, and B10) do not exhibit knickzones along their profile. We instead correlate the knickzones to factors other than eustasy—tectonic (B2, B3, B5, B6, B7, B8, B13, B14, B15, B16) or lithologic (B9, B11, B12, B7, B8).

[44] In the southern part of the peninsula, channels B11 and B12 show a concave profile upslope and a more convex profile downslope (Figure 6). This change can be explained by the effect of lithologic contrast between resistant igneous rocks (gabbro) downslope and more erodible volcano-sedimentary rocks upslope (Figure 6). For B12, we also suspect that sea cliff erosion may affect the lowest part of this profile shape. Anomalously, however, channel profiles B7–B9 and B13 are convex, where the basins incise soft formations (alluvial sediments, weathered ophiolite, volcanic sediments). As all these streams drain the Cape Kamchatsky massif, these anomalies can be interpreted as morphometric evidence of a more rapid rate of uplift in this massif. We already suspected this uplift due to the radial drainage network of the Cape Kamchatsky massif, and it was also highlighted by *Gaedicke et al*. [2000] from the presence of Quaternary marine formations at high altitude and by *Freitag et al*. [2001] from fission track analysis of exhumation rates.

[45] Concerning the drainage of B13 (Pikezh River), the impact of vertical displacement of a fault zone in the valley could explain the knickzone in the profile upslope of the fault crossing the valley (Figure 6). The same is also the case for B14 (first Pereval'naya River) and for streams B6 and B15 (second Pereval'naya River valley), which intersect the 1PNRFZ and the 2PNRFZ, respectively. For each of these channels, the knickzones do not correspond to lithologic changes.

[46] Uplift of the Cape Reef massif as revealed by marine terrace analysis is also highlighted by upslope knickzones along stream profiles B5 and B16. These anomalies are not associated with lithologic contrast or fault/drainage intersections, and thus, we interpret them to be induced by a general uplift of the zone by tilting.

[47] The impact of fault F3 and the associated bulge of Cape Sivuchy (Figure 6) are also suggested by the knickzones upslope of the fault along channel profiles B2 and B3, which drain the southern slope of the bulge. The knickzone alignment is parallel to the bulge axis. However, the streams that drain the northern slope (B20, B19, B18) do not show anomalies along their concave-up long profile as might be expected by symmetry. A hypothesis to explain this difference is that marine erosion on the northern side has removed the convex reach of the channel profile. This explanation may also apply to B17 and B21.

4.3.3. Hypsometric Parameters

[48] The area below a hypsometric curve portrays the amount of material left after erosion. A low hypsometric integral (H*I* <0.5) indicates major erosional activity and, thus, a mature basin [*Stralher*, 1952; *Hurtrez et al*., 1999]. Except for the alluvial basin B11 (Figure 6), the hypsometric integrals of the 20 other selected basins have generally moderate to low values (H*I* <0.5) reflecting a dissected, eroding landscape, approaching equilibrium phase. The low H*I* values (H*I* <0.5) may be explained by the easily eroded lithology of soft volcaniclastic and alluvial deposits underlying most the peninsula. Resistant igneous basement crops out only in the southern region and explains the highest integrals of basins B10–B12 (Figure 6).

[49] There are some patterns unexplained by erodability, however. In the south, the high values of basins B8, B13, and B14 which drain only soft formations require another factor such as tectonic uplift (Figure 6). In contrast, basins B4–B6 and B16 in the central region have very low H*I* values (< 0.2) that cannot be explained by the easily eroded lithology of soft volcaniclastic and alluvial deposits alone but by the additional effect of the geomorphic and structural location of the basins. The basins drain, in major part, large alluvial plains located in the suspected NE-SW trending syncline between the zones of Cape Reef and Cape Sivuchy (Figures 6 and 7). This region may be subsiding and thus preventing efficient erosion. The northern basins (B17–B21) show moderate values of H*I* relative to the other basins on the peninsula. As these northern basins drain soft formations (Paleogene sandstone and tuff), the increase in H*I* values compared with those of the central zone may be explained by the tectonic bulge effect in this region from Stolbovoe Lake to Cape Sivuchy (Figure 6).

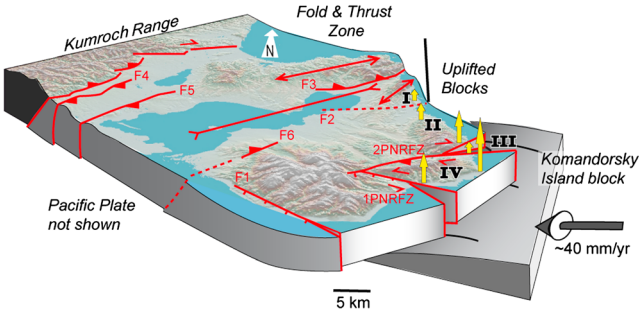

Figure 7. Cartoon representing the "encroachment" of the Komandorsky Island block on the Kamchatsky Peninsula.

5. Discussion

5.1. Active Deformation of the Coastal Sequences and Onshore/Offshore Fault Correlation

[50] For all four zones defined above, relative differences in altitude are conserved between the oldest (highest) Holocene shoreline angle and the youngest (lowest) Pleistocene shoreline angle (Figure 3 for uplift rates). Morphologically, the sequences (particularly the Pleistocene ones) are often tilted. These vertical motions are accommodated by faults at the boundary of each zone (which behaves as block), from north to southwest: F3, F2, the northern fault of the 2PNRFZ, the southern fault of the 2PNRFZ, and F6 (Figures 3 and 6). Some faults oblique to the tilting direction are observable in the landscape at the outcrop scale and in aerial views, but fault planes and slickensides are not noticeable because they are covered by alluvial and soil-tephra deposits.

[51] The fault system of the offshore Aleutian-Komandorsky transform boundary is trending toward the Kamchatsky Peninsula and these onshore blocks and faults. *Freitag et al*. [2001] and *Gaedicke et al*. [2000] interpreted the onshore coastal faults (1PNRFZ, 2PNRFZ, F2) as prolongations of offshore dextral transform faults which exhibit reverse dextral motion due to bent terminations of the faults toward shore. They take this interpretation to argue for the hypothesis of impingement of the Komandorsky Island block. For *Kozhurin* [2007], active onshore faults on the peninsula may reflect just internal deformation in the peninsula induced by its clockwise rotation associated with the decrease in rate of dextral motion from one fault to another with distance (northward) from the Aleutian-Pacific interface. The disagreements are partly based on differences in field interpretations and partly on differences in how those interpretations fit the larger picture.

[52] To the north, we show folding and vertical motion associated with the ENE trending F3 that bounds Zone I. These trends agree with the SE verging reverse kinematics assigned to this fault by *Freitag et al*. [2001]. However, the strike is perpendicular to the offshore transform fault zone, which does not permit a linking of the two structures.

[53] South of Zone I, as in *Kozhurin* [2007] and *Gaedicke et al*. [2000], we suspect a ENE trending fault (F2). However, we did not observe any displacements of Quaternary geomorphological features along the fault. Thus, dextral motion or reverse motion inferred by *Kozhurin* [2007] or *Gaedicke et al*. [2001], respectively, is still subject to discussion. We do not have any argument to link this fault to an offshore fault.

[54] Zone III, where the second Pereval'naya River valley is located, is bounded by the northern and southern faults of the 2PNRFZ. Apparently, vertical fault motion is tilting and offsetting the terrace sequences north and south of the 2PNRFZ, within which the terrace sequence is lower (Figure 3). The structural trough between the northern and southern faults could correspond to a foreland basin if the boundary faults accommodate shortening or a graben if the faults accommodate extension. However, we also have to

keep in mind that we observed horizontal offsets of the marine terraces which are higher than the vertical offsets along the southern fault of the 2PNRFZ, indicating that dextral motion is the dominant component of fault slip in this fault zone, in agreement with *Kozhurin* [2007]. Along the southern fault of the 2PNRFZ, *Kozhurin* [2007] measured right-lateral displacements of Holocene geomorphic markers and estimated a ~25 mm/yr horizontal slip rate. According to the horizontal offset and age of T1, we estimate a horizontal slip rate of ~10 mm/yr.

[55] South of the 2PNRFZ, the MIS 5e marine terrace exhibits its maximum elevation (Cape Africa block, Zone IV). According to the marine terrace offset, the vertical slip rate is higher along the southern fault of the 2PNRFZ than along the northern fault of the 2PNRFZ. The asymmetry in uplift and tilt rates north and south of the 2PNRFZ leads us to interpret that the excess uplift to the south is due to the simultaneous activity of the 2PNRFZ and the 1PNRFZ bounding the Cape Africa block, producing a bulge effect on this block (Figure 6).

[56] A connection of the 2PNRFZ with a proposed splay of the offshore Bering fault [*Gaedicke et al*., 2000] is supported by their proximity, their similar dextral kinematics, and the small angle between their strike which can produce a small reverse motion component along the 2PNRFZ, explaining the maximum uplift of the northern part of Africa block. Thus, our results are not only in agreement with the kinematics proposed by *Kozhurin* [2007] for the 2PNRFZ, but they are also in agreement with the offshore/onshore fault connection proposed by *Gaedicke et al*. [2000].

[57] Concerning the 1PNRFZ south of Zone IV and north of Cape Kamchatsky, according to our data, we have observed a vertical motion along the 1PNRFZ associated with a northern uplifted flank of the fault. This vertical motion disagrees with dextral motion proposed by *Gaedicke et al*. [2000] and *Freitag et al*. [2001] but is consistent with the south verging normal faulting attributed to the 1PNRFZ by *Kozhurin* [2007]. *Freitag et al*. [2001] and *Gaedicke et al*. [2000] proposed dextral kinematics with a reverse bend termination westward. Their dextral tectonic regime was deduced by observation of right-lateral striations on Pliocene deposits along the main SE trending fault on the coast. They considered then that the fault is the prolongation of the offshore dextral Pikezh fracture zone. Instead, *Baranov et al*. [2010] attributed a sinistral motion to the same fault according to left-lateral offsets of minor drainages. *Kozhurin* [2007] considered the entire 1PNRFZ to be largely normal and dipping to the south with a small component of left-lateral motion. Indices of normal faulting are purely geometric, reflecting the interaction between topography and the fresh fault scarp orientation, if it corresponds to the fault plane. Kozhurin concluded that contrary to previous interpretations, there are still no valid data supporting the idea that the fault zone corresponds to the dextral offshore Pikezh fault zone. Furthermore, sinistral offset of drainages shown by *Baranov et al*. [2010] is convincing enough for us to favor a sinistral transtensive tectonic regime for the 1PNRFZ that does not allow its link to the dextral offshore Pikezh fault zone.

[58] West of Cape Kamchatsky, an inferred NW-SE trending active fault bounding the major relief (F6) is interpreted in this study as a normal fault. Ten kilometers southwest of fault F6, the major NW-SE trending Steller fracture zone affects the offshore domain (Figure 2). This NW-SE trending fault zone was interpreted by *Gaedicke et al*. [2000] as a sinistral strike-slip fault because it left-laterally displaces the Kamchatka River canyon and is associated with NNW-SSE anticlines and reverse faults. As the NNW trending F6 fault is located close to the NW trending Steller FZ, it could represent a splay off this major structure. However, its normal fault kinematics is not consistent with the reverse sinistral kinematics that would be observed along a NNW trending splay of the NW trending sinistral Steller fault zone. Thus, we do not connect this onshore fault with the offshore neighboring fault.

5.2. Deformation Rate and Active Tectonics on the Northwestern Terminus of the Pacific Plate

[59] Drainage anomalies combined with analyses of uplifted marine terraces and fault scarps in Quaternary deposits allow us to distinguish four coastal blocks delimited by onshore faults: the Cape Kamchatsky block, the Cape Africa block, the second Pereval'naya River valley block, and the Cape Reef block, which are uplifted and tilted with different uplift rates (Figures 3 and 7). As observed elsewhere on very active areas of the Pacific Rim, the uplift rates are highly variable [*Ota and Yamaguchi*, 2004]. Landward of (behind) these blocks, compressive deformation creates NE-SW reverse faults and NE trending bulges interpreted as anticlines.

[60] The most intense deformation takes places in Cape Africa, where the block constitutes a corner that is pushed against the Kamchatsky Peninsula due to dextral motion along the 1PNRFZ and sinistral motion along the conjugate 2PNRFZ (Figures 3 and 7). This analysis is in agreement with kinematics suggested by *Kozhurin* [2007] and *Baranov et al*. [2010]. The coastal sequence in this area reflects strong uplift rates (locally >2 mm/yr). The impingement of the Cape Africa block should be also accommodated by shortening associated with a component of reverse motion along the 2PNRFZ as suggested by *Gaedicke et al*. [2000].

[61] To the southwest of Cape Africa, Holocene marine terraces are present at the southern point of Cape Kamchatsky, but Pleistocene ones are not observable in the landscape. There are two possible explanatory hypotheses: (1) The Pleistocene terraces were never carved; or 2) the terraces were carved but erased after their formation. The first hypothesis would imply that the uplift there is a recent phenomenon. However, because of the lithology of the Cape Kamchatsky block (i.e., in most cases, fine-grained deposits of the Olkhovskaya Formation), we favor the second hypothesis. Pleistocene marine terraces do crop out along the southwestern part of the Cape Kamchatsky block, and alluvial fans above them seem to be affected by a NW-SE trending normal fault (F6) which can accommodate uplift. For its part, the reverse motion along F1 bounding the northwestern part of the Cape Kamchatsky block could accommodate the shortening produced by the westward motion of this block (Figures 2 and 7).

[62] To the north of Cape Africa, the Cape Reef block shows an extensive sequence of marine terraces (Figure 3). They are tilted northward in relation with the vertical motion along the 2PNRFZ. The asymmetric basin that drains the

western side of Cape Reef suggests a westward component of tilting. Combining the two vergences of tilting, Cape Reef, with a rigid behavior, tilts toward the NW (Figure 7). This strike agrees with the motion of the frontal impingement of the Komandorsky Island block against Kamchatka.

[63] In the northwestern part of the Peninsula, we detected recent compressive structures: to the west, NE-SW reverse faults and, to the east, NE-SW folds extended to the south of Cape Nose (Figure 6). This region corresponds to a fold-and-thrust zone (Figure 7). One of these faults was trenched by *Kozhurin* [2009] for paleoseismicity study and reveals minor reverse NW verging faults affecting alluvial deposits. The Stolbovoe, Kultuchnoe, and Nerpich'e Lakes are located on a NE-SW depression corresponding to a syncline delimited by reverse faults and anticlines (Figure 7).

[64] All these results support the active Aleutian-Komandorsky arc collision suggested by a number of earlier studies (reviewed in *Scholl* [2007]). Uplifted and deformed terraces as well as distinctive drainage patterns demonstrate that collision affects the whole Kamchatsky Peninsula (Figure 7), uplifting coastal blocks and folding the hinterland as a "bulldozer effect." Deformation reaches the Kumroch Range which was formed during the late Miocene collision between the Kronotskaya arc and Kamchatka [*Solov'ev et al*., 2004]. This range shows active reverse faulting in its eastern boundary only in the Kamchatsky Peninsula region [*Kozhurin*, 2009]. Westward motion of the Kamchatsky Peninsula due to the Aleutian-Komandorsky arc collision is indicated also by the sinistral motion along the Steller fault zone west of the Pacific subduction zone. The Steller fault zone delimits to the south the Aleutian-Komandorsky island block and the Kamchatsky Peninsula. Local sinistral motion accommodates the westward relative movement of the peninsula relative to the accretionary wedge west of the Pacific subduction zone due to the arc-continent collision [*Geist and Scholl*, 1994; *Gaedicke et al*., 2000].

[65] *Kozhurin* [2007] suggested that the Kamchatka-Aleutian interaction produces only clockwise rotation of the entire Kamchatsky Peninsula block accommodated by movements along onshore faults. Such a model does not predict folding and reverse faulting as identified in our study for faults F1, F3, F4, and F5, with mainly dextral kinematics along F3, F2, and 2PNRFZ and normal kinematics along 2PNRFZ, F4, and F5. In a collision context, block rotation would be blocked by shortening [*England and Molnar*, 1990]. We do not reject the occurrence of potential block rotation of the entire Kamchatsky Peninsula proposed by *Kozhurin* [2007], but most of the kinematics of internal faults he deduced disagree with our results; moreover, if the rotation exists, compressive contact with the Kumroch Range to the west must slow down this rotation.

6. Conclusion

[66] Our results show marked tectonic segmentation of the coastal fringe of the Kamchatsky Peninsula. Late Pleistocene uplift rates along the coast vary in space with marked rapidity, ranging from 0.2 to 2.74 mm/yr. Geomorphic analysis suggests folding and thrusting in the hinterland of the Kamchatsky Peninsula and tilting of the coastal blocks associated with vertical and strike-slip displacements along faults at the block boundaries. Since the Kamchatsky Peninsula is located near the western end of the large dextral transform system associated with the western Aleutian-Komandorsky arc, the structures on the peninsula likely accommodate westward convergence of the Komandorsky Island block and its collision with the continent, producing the effect of a bulldozer.

[67] This deformation pattern indicates that the Kamchatsky Peninsula actively undergoes arc-continent collision with the Aleutian arc at the triple junction between the Okhotsk, North American, and Bering plates, as suggested by several earlier studies. On the other hand, the pattern, in particular the shortening in the hinterland associated with Kumroch Range blocking, contravenes an active, rigid, clockwise rotation of the entire Kamchatsky Peninsula as proposed by *Kozhurin* [2007]. Also, the connection between onshore faults of the peninsula and offshore faults of the Aleutian-Komandorsky transform boundary suggested by *Gaedicke et al*. [2000] is not supported by our results, except for the fault zone of the second Pereval'naya River valley, which can be linked to a proposed splay of the Bering fault zone. This independence of onshore faults was also proposed by *Kozhurin* [2007], although our kinematic model does not agree with some details of his analysis.

[68] In this study, uplift rates and active deformation of the Kamchatsky Peninsula—located at the intersection of the Pacific subduction zone and the Komandorsky-Aleutian dextral transform boundary—have been estimated using a combined field and map analysis of Pleistocene marine terraces, drainage anomalies, and active faults. Extensive field data and ground truthing accompanied by morphotectonic analysis using several remote-sensing techniques have permitted us to refine a neotectonic model for the entire Kamchatsky Peninsula as affected by this very active and complex collision zone.

[69] **Acknowledgments.** We thank Viktor Morosov for field assistance. The research was supported by grant EAR-0125787 (to J. Bourgeois) from the U.S. National Science Foundation. A final version of this manuscript was completed during a visit of J. Bourgeois to the University of Caen supported by the Professeur Invité programme of the University of Caen. The paper is dedicated to the memory of Katya Kravchunovskaya.

References

Alexeiev, D. V., C. Gaedicke, N. Tsukanov, and R. Freitag (2006), Collision of the Kronotskiy arc at the NE Eurasia margin and structural evolution of the Kamchatka-Aleutian junction, *Int. J. Earth Sci.*, *95*, 977–993, doi:10.1007/978-3-540-88558-0_9.

Apel, E. V., G. M. Bürgmann, G. M. Steblov, N. F. Vasilenko, and R. W. King (2006), Independent active microplate tectonics of northeast Asia from GPS velocities and block modeling, *Geophys. Res. Lett.*, *33*, L11303, doi:10.1029/2006GL026077.

Bakhteev, M. K., O. A. Morozov, and S. R. Tikhomirova (1992), Paragenesis of Late Cenozoic structures of the Kuril-Kamchatka-Aleutian Island Arc juncture zone [in Russian], Higher Education Institution News, Geol. Exploring 3, 18–25.

Bakhteev, M. K., O. A. Morozov, and S. R. Tikhomirova (1993), Structure and age of serpentinite melange of the Kamchatsky Cape Peninsula (eastern Kamchatka) [in Russian], Higher Education Institution News, Geol. Exploring 3, 23–28.

Baranov, B. V., C. Gaedicke, R. Freitag, and K. A. Dozorova (2010), Active faults of the south eastern Kamchatky peninsula and Komandorsky shear zone [in Russian], Bull. Kamchatka Reg. Assoc. "Educ.-Sci. Cent.", *Earth Sci.*, *16*, 66–77.

Basilyan, A. E., and M. E. Bylinskaya (1997), Shelf of Kamchatka Peninsula (eastern Kamchatka) in Late Pliocene-Early Quaternary (Olkhovskoe time): Stratigraphy, *Geol. Correlations*, *5*, 83–92.

Berryman, K. (1993a), Distribution, age, and deformation of the late Pleistocene marine terraces at Mahia Peninsula, Hikurangi subduction margin, New Zealand, *Tectonics*, *12*, 1365–1379, doi:10.1029/93TC01543.

Berryman, K. (1993b), Age, height, and deformation of Holocene marine terraces at Mahia Peninsula, Hikurangi subduction margin, New Zealand, *Tectonics*, *12*, 1347–1364, doi:10.1029/93TC01542.

Bishop, P., T. B. Hoey, J. D. Jansen, and I. L. Artza (2005), Knickpoint recession rate and catchment area: The case of uplifted rivers in eastern Scotland, *Earth Surf. Processes Landforms*, *30*, 767–778, doi:10.1002/esp.1191.

Bourgeois, J., T. Pinegina, V. Ponomareva, and N. Zaretskaia (2006), Holocene tsunamis in the southwestern Bering Sea, Russian Far East, and their tectonic implications, *Geol. Soc. Am. Bull.*, *118*, 449–463, doi:10.1130/B25726.1.

Bull, W. B. (1985), Correlation of flights of global marine terraces, in 15th Annual Geomorphology Symposium, edited by M. Morisawa and J. Hack, pp. 129–152, State Univ. of New York at Binghamton, Hemel Hempstead.

Burbank, D., and R.-S. Anderson (2001), *Tectonic Geomorphology*, 274 pp., Wiley-Blackwell, Hoboken, N.J.

Bürgmann, R., M. G. Kogan, G. M. Steblov, G. Hilley, V. E. Levin, and E. V. Apel (2005), Interseismic coupling and asperity distribution along the Kamchatka subduction zone, *J. Geophys. Res.*, *110*, B07405, doi:10.1029/2005JB003648.

Chappell, J. (1974), Geology of coral terraces, Huon Peninsula, New Guinea: A study of Quaternary tectonic movements and sea-level changes, *Geol. Soc. Am. Bull.*, *85*, 553–570, doi:10.1130/0016-7606(1974)85<553:GOCTHP>2.0.CO;2.

Cox, R. T. (1994), Analysis of drainage basin symmetry as a rapid technique to identify areas of possible Quaternary tilt-block tectonics: An example of the Mississippi embayment, *Geol. Soc. Am. Bull.*, *106*, 571–581, doi:10.1130/0016-7606(1994)106<0571:AODBSA>2.3.CO;2.

Cross, R. S., and J. T. Freymueller (2008), Evidence for and implications of a Bering plate based on geodetic measurements from the Aleutians and western Alaska, *J. Geophys. Res.*, *113*, B07405, doi:10.1029/2007JB005136.

Delcaillau, B., B. Deffontaines, L. Floissac, J. Angelier, J. Deramond, P. Souquet, H. T. Chu, and J. F. Lee (1998), Morphotectonic evidence from lateral propagation of an active frontal fold; Pakuashan anticline, foothills of Taiwan, *Geomorphology*, *24*, 263–290. doi:10.1016/S0169-555X(98)00020-8.

DeMets, C., R. G. Gordon, D. F. Argue, and S. Stein (1994), Effect of recent revisions to the geomagnetic reversal time scale on estimates of current plate motions, *Geophys. Res. Lett.*, *21*, 2191–2194.

Duvall, A., E. Kirby, and D. Burbank (2004), Tectonic and lithologic controls on bedrock channel profiles and processes in coastal California, *J. Geophys. Res.*, *109*, F03002, doi:10.1029/2003JF000086.

England, P., and P. Molnar (1990), Right-lateral shear and rotation as explained for strike-slip faulting in the eastern Tibet, *Nature*, *344*, doi:10.1038/344140a0.

Erlikh, E. N., I. V. Melekestsev, and A. E. Shantser (1974), Neotectonica [in Russian], in *Kamchatka, Kuril and Kommander Islands*, edited by J. V. Luchitskiy, pp. 345–368, Nauka, Moscow.

Fedorenko, S. I. (1965), Marine terrace of the eastern coast of Kamchatka [in Russian], *Bull. Moscow Soc. Nat.*, Geol. Dep., *XL*, 80–90.

Freitag, R., C. Gaedicke, B. Baranov, and N. Tsukanov (2001), Collisional processes at the junction of the Aleutian-Kamchatka arcs: New evidence from fission track analysis and field observations, *Terra Nova*, *13*, 433–442, doi:10.1046/j.1365-3121.2001.00375.x.

Gaedicke, C., B. Baranov, N. Seliverstov, D. Alexeiev, N. Tsukanov, and R. Freitag (2000), Structure of an active arc-continent collision area: The Aleutian-Kamchatka junction, *Tectonophysics*, *325*, 63–85, doi:10.1016/S0040-1951(00)00131-1.

Gardner, T. W. (1983), Experimental study of knickpoint and longitudinal evolution in cohesive, homogeneous material, *Geol. Soc. Am. Bull.*, *94*, 664–672, doi:10.1130/0016-7606(1984)95<123:ESOKAL>2.0.CO;2.

Geist, E. L., and D. W. Scholl (1994), Large-scale deformation related to the collision of the Aleutian Arc with Kamchatka, *Tectonics*, *13*, 538–560, doi:10.1029/94TC00428.

Gordeev, E. I., A. A. Gusev, V. E. Levin, V. F. Bakhtiarov, V. M. Pavlov, V. N. Chebrov, and M. Kasahara (2001), Preliminary analysis of deformation at the Eurasia-Pacific-North America plate junction from GPS data, *Geophys. J. Int.*, *147*, 189–198, doi:10.1046/j.0956-540x.2001.01515.x.

Hack, J. T. (1973), Stream-profile analysis and stream gradient index, *J. Res. U.S. Geol. Surv.*, *1*, 421–429.

Hare, P. H., and T. W. Gardner (1985), Geomorphic indicators of vertical neotectonism along converging plate margins, Nicoya Peninsula, Costa Rica, in *Tectonic Geomorphology*, edited by M. Morisawa and J. T. Hack, pp. 75–104, Allen and Unwin, Boston, Mass.

Hurtrez, J. E., C. Sol, and F. Lucazeau (1999), Effects of drainage area on hypsometry from analysis of small-scale drainage basins in the Siwaliks Hills (Central Nepal), *Earth Surf. Processes Landforms*, *29*, 799–808, doi:10.1002/(SICI)1096-9837(199908)24:9<799::AID-ESP12>3.0.CO;2-4.

James, N. P., E. W. Mountjoy, and A. Omura (1971), An early Wisconsin reef terrace at Barbados, West Indies, and its climatic implications, *Geol. Soc. Am. Bull.*, *82*, 2011–2017, doi:10.1130/0016-7606(1971)82[2011:AEWRTA]2.0.CO;2.

Johnson, M. E., and L. K. Libbey (1997), Global review of upper Pleistocene (substage 5e) rocky shores: Tectonic segregation, substrate variation, and biological diversity, *J. Coastal Res.*, *13*, 297–307.

Keller, E. A., and N. Pinter (2002), *Active Tectonics: Earthquakes, Uplift and Landscape*, 362 pp., Prenctice Hall, Upper Saddle River, N.J.

Kimura, G. (1996), Collision orogeny at arc-arc junctions in the Japanese Islands, *Isl. Arc*, *5*, 262–275, doi:10.1111/j.1440-1738.1996.tb00031.x.

Kirby, E., and K. Whipple (2001), Quantifying differential rock-uplift rates via stream profile analysis, *Geology*, *29*, 415–418. doi:10.1130/0091-7613(2001).

Konstantinovskaia, E. A. (2000), Geodynamics of an early Eocene arc-continent collision reconstructed from the Kamchatka Orogenic Belt, NE Russia, *Tectonophysics*, *325*, 87–105, doi:10.1016/S0040-1951(00)00132-3.

Konstantinovskaia, E. A. (2001), Arc-continent collision and subduction reversal in the Cenozoic evolution of the Northwest Pacific: An example from Kamchatka (NE Russia), *Tectonophysics*, *333*, 75–94, doi:10.1016/S0040-1951(00)00268-7.

Kozhurin, A. N. (1985), Quaternary tectonics of the Kumroch range and the Kamchatsky peninsula (eastern Kamchatka), *Geotectonica*, *2*, 76–87.

Kozhurin, A. I. (2004), Active faulting at the Eurasian, North American and Pacific plates junction, *Tectonophysics*, *380*, 273–285, doi:10.1016/j.tecto.2003.09.024.

Kozhurin, A. I. (2007), Active faulting in the Kamchatsky Peninsula, Kamchatka-Aleutian junction, in *Volcanism and Subduction: The Kamchatka Region*, *Geophys. Monogr. Ser.*, vol. 172, edited by J. Eichelberger et al., pp. 263–282, AGU, Washington, D. C.

Kozhurin, A. I. (2009), A dangling slab and arc-normal extension: The case of Kamchatka, Russia, Abstract T41C-2034 presented at 2009 Fall Meeting, AGU, San Francisco, Calif., 14–18 Dec.

Lajoie, K. R. (1986), Coastal tectonics, in *Active Tectonics*, pp. 95–124, Natl. Acad. Press, Washington, D. C.

Lander, A. V., B. G. Bukchin, A. V. Kiryushin, and D. V. Droznin (1996), The tectonic environment and source parameters of the Khailino, Koryakiya earthquake of March 8, 1991: Does a Beringia plate exist?, *Comput. Seismol. Geodyn.*, *3*, 80–96.

Lees, J. L., J. Vandecar, E. I. Gordeev, A. Ozerov, M. T. Brandon, J. Park, and V. E. Levin (2007), Three-dimensional images of the Kamchatka-Pacific plate cusp, in *Volcanism and Subduction: The Kamchatka Region*, *Geophys. Monogr. Ser.*, vol. 172, edited by J. Eichelberger et al., pp. 65–75, AGU, Washington, D. C.

Levin, V., M. N. Shapiro, J. Park, and M. H. Ritzwoller (2005), Slab portal beneath the western Aleutians, *Geology*, *33*, 253–256, doi:10.1130/G20863.1.

Mackey, K. G., K. Fujita, L. V. Gunbina, V. N. Kovalev, V. S. Imaev, B. M. Koz'min, and L. P. Imaeva (1997), Seismicity of the Bering Strait region: Evidence for a Bering block, *Geology*, *25*, 979–982, doi:10.1130/0091-7613(1997)025<0979:SOTBSR>2.3.CO;2.

Mackey, K. G., et al. (2010), Seismicity map of eastern Russia, 1960–2010, *Seismol. Res. Lett.*, *81*, 761–768.

McElfresh, S. B. Z., W. Harbert, C.-Y. Ku, and J.-S. Lin (2002), Stress modeling of tectonic blocks at Cape Kamchatka, Russia using principal stress proxies from high-resolution SAR: New evidences for the Komandorskiy block, *Tectonophysics*, *354*, 239–256, doi:10.1016/S0040-1951(02)00341-4.

Merritts, D., and K. R. Vincent (1989), Geomorphic response of coastal streams to low, intermediate, and high rates of uplift, Mendocino Triple Junction region, Northern California, *Geol. Soc. Am. Bull.*, *110*, 1373–1388, doi:10.1130/0016-7606(1989)101<1373:GROCST>2.3.CO;2.

Molin, P., F. J. Pazzaglia, and F. Dramis (2004), Geomorphic expression of active tectonics in a rapidly-deforming forearc, Sila Massif, Calabria, Southern Italy, *Am. J. Sci.*, *204*, 559–589, doi:10.2475/ajs.304.7.559.

Ota, Y. (1986), Marine terraces as reference surfaces in late Quaternary tectonics studies: Examples from the Pacific Rim: New Zealand, *N. Z. J. Geol. Geophys.*, *24*, 357–375.

Ota, Y., and M. Yamaguchi (2004), Holocene coastal uplift in the Western Pacific Rim in the context of the Late Quaternary uplift, *Quat. Int.*, *120*, 105–117, doi:10.1016/j.quaint.2004.01.010.

Pedoja, K., J. Bourgeois, T. Pinegina, and B. Higman (2006), Does Kamchatka belong to North America? An extruding Okhotsk block suggested by coastal neotectonics of the Ozernoi Peninsula, Kamchatka, Russia, *Geology*, *34*, 353–356, doi:10.1130/G22062.1.

Pedoja, K., et al. (2011), Relative sea-level fall since the last interglacial stage: Are coasts uplifting worldwide?, *Earth-Sci. Rev.*, *108*, 1–15.

Pevzner, M. M., V. Ponomareva, and I. V. Melekestsev (1997), Chernyi Yar—A datum section of Holocene marker tephra of the northeastern coast of Kamchatka, *Volcanol. Seismol.*, *4*, 3–18.

Pflanz, D., C. Gaedicke, R. Freitag, M. Krbetschek, N. Tsukanov, and B. Baranov (2012), Neotectonics and recent uplift at Kamchatka and Aleutian arc junction, Kamchatka Cape area, NE Russia, *Int. J. Earth Sci.*, 1–14.

Pinegina, T., E. A. Kravchunovskaya, A. V. Lander, A. I. Kozhurin, J. Bourgeois, and E. M. Martin (2010), Holocene vertical movement of Kamchatsky Peninsula coast (Kamchatka) based on studies of marine terraces, Bull. Kamchatka Reg. Assoc. "Educ.-Sci. Cent.", Earth Sci., *1*, 231–247.

Pinegina, T., J. Bourgeois, E. A. Kravchunovskaya, M. Arcos, A. V. Lander, K. Pedoja, and E. M. Martin (2013), A nexus of plate interaction: Segmented vertical movement of Kamchatsky Peninsula (Kamchatka) based on Holocene aggradational marine terraces, *Geol. Soc. Am. Bull.*, doi:10.1130/B30793.1, in press.

Ponomorova, V., P. Kyle, M. Pevzner, L. Sulerzhitsky, and M. Hartman (2007), Holocene eruptive history of Shiveluch Volcano, Kamchatka Peninsula, Russia, in *Volcanism and Subduction: The Kamchatka Region*, *Geophys. Monogr. Ser*., vol. 172, edited by J. Eichelberger et al., pp. 263–282, AGU, Washington, D. C.

Regard, V., R. Lagnous, N. Espurt, J. Darrozes, P. Baby, M. Roddaz, Y. Calderon, and W. Hermoza (2009), Geomorphic evidence for recent uplift of the Fitzcarrald Arch (Peru): A response to the Nazca Ridge subduction, *Geomorphology*, *107*, 107–117, doi:10.1016/j.geomorph.2008.12.003.

Scholl, D. W. (2007), Viewing the tectonic evolution of the Kamchatka-Aleutian (KAT) connection with an Alaska crustal extrusion perspective, in *Volcanism and Subduction: The Kamchatka Region*, *Geophys. Monogr. Ser.*, vol 172, edited by J. Eichelberger et al., pp. 3–35, AGU, Washington, D. C.

Seliverstov, N. (1983), The structure of Kuril-Kamchatka and Aleutian Islands according to single-channel seismic data [in Russian], *Volcanol. Seismol.*, *2*, 53–67.

Seliverstov, N. (1998), The bottom structure near East Kamchatka and geodynamics of the junction zone of the Kuril-Kamchatka and Aleutian island arcs: Moscow [in Russian], *Sci. World*, 164 pp.

Seliverstov, N. (2009), Geodynamical zonation of the Kuril-Kamchatka and Aleutian island arc: Petropavlosk–Kamchatskii [in Russian], *Russ. Acad. Sci.*, 191 pp.

Shapiro, M. N., and A. V. Solov'ev (2009), Formation of the Olyutorsky-Kamchatka foldbelt: A kinematic model, *Russ. Geol. Geophys.*, *50*, 668–681, doi:10.1016/j.rgg.2008.10.006.

Solov'ev, A. V., M. N. Shapiro, J. E. Garver, and A. V. Lander (2004), Formation of the east Kamchatkan accretionary prism according to fission-track dating of Zircons from terrigene rocks, *Geol. Geofiz.*, *45*, 1292–1302.

Steblov, G. M., and M. G. Kogan (2005), Strain accumulation and strain partitioning in the Western Aleutian subduction zone, Abstract T42A-08 presented at 2005 Fall Meeting, AGU, San Francisco, Calif., 5–9 Dec.

Stralher, A. N. (1952), Hypsometric analysis of erosional topography, *Geol. Soc. Am. Bull.*, *63*, 1117–1142, doi:10.1130/0016-7606(1952)63[1117:HAAOET]2.0.CO;2.

Tsukanov, N. V. (1991), Tectonic evolution of Kamchatka peri-oceanic area in the Late Mesozoic and Early Cenozoic [in Russian], Dokl. Acad. Sci. USSR, *462*, 1–104.

Whipple, K. X., and G. E. Tucker (1999), Dynamics of the stream-power river incision model: Implications for height limits of mountain ranges, landscape response timescales, and research needs, *J. Geophys. Res.*, *104*, 661–674, doi:10.1029/1999JB900120.

Zaprowski, B. J., E. B. Evenson, F. J. Pazzaglia, and J. B. Epstein (2001), Knickzone propagation in the Black Hills and northern High Plains: A different perspective on the late Cenozoic exhumation of the Laramide Rocky Mountains, *Geology*, *29*, 547–550, doi:10.1130/0091-7613(2001)029<0547:KPITBH>2.0.CO;2.

Zazo, C. (1999), Interglacial sea levels, *Quat. Int.*, *55*, 101–113.